



Project Summary

Chlorine Absorption in S(IV) Solutions

Sharmistha Roy and Gary T. Rochelle

The rate of chlorine (Cl_2) absorption into aqueous sulfite/bisulfite [S(IV)] solutions was measured at ambient temperature using a highly characterized stirred-cell reactor. The reactor media were 0 to 10 mM S(IV) with pH ranging from 3.5 to 8.5. Experiments were performed using 20 to 300 ppm Cl_2 in nitrogen (N_2) or in air. Chlorine absorption was modeled using the theory of mass transfer with chemical reaction. Chlorine reacts quickly with S(IV) to form chloride and sulfate. Chlorine absorption is enhanced by increasing pH and S(IV) concentration. The rate constant for the reaction of Cl_2 with S(IV) was too rapid to be precisely measured using the existing stirred-cell reactor, due to mass transfer limitations. However, the most probable value of the rate constant was determined to be $2 \times 10^9 \text{ L/mol}\cdot\text{s}$.

These results are relevant in the simultaneous removal of Cl_2 , sulfur dioxide (SO_2), and elemental mercury (Hg) from flue gas. The developed model shows that good removal of both Cl_2 and Hg should be possible with the injection of 1 to 10 ppm Cl_2 to an existing limestone slurry scrubber. These results may also be applicable to scrubber design for removal of Cl_2 in the pulp and paper and other industries.

This Project Summary was developed by the National Risk Management Research Laboratory's Air Pollution Prevention and Control Division, Research Triangle Park, NC, to announce key findings of the research project that is fully documented in a separate report of the

same title (see Project Report ordering information at back).

Introduction

Mercury (Hg) pollution is an important problem because of its behavior in the environment (bioaccumulation) and the potential for deleterious health effects. Roughly 85% of anthropogenic Hg emissions are from combustion sources. The flue gas from these sources contains sulfur dioxide (SO_2) and hydrogen chloride (HCl) at much higher concentrations than the Hg compounds. Aqueous scrubbing is currently used to remove SO_2 and HCl from these flue gases. It should be possible to remove Hg by conventional scrubbing technologies with the addition of reagents to produce chlorine (Cl_2), which will oxidize the Hg to a more soluble form through reaction in the mass transfer boundary layer.

Mercury reacts with Cl_2 to form mercuric chloride (HgCl_2) which is very soluble and can thus be easily removed through aqueous scrubbing. The Hg must react with the Cl_2 before the Cl_2 gets reduced by the dissolved SO_2 present as aqueous sulfite/bisulfite [S(IV)]. S(IV) represents sulfurs in the +4 oxidation state (sulfite and bisulfite). Therefore, the kinetics of the reaction between Cl_2 and S(IV) needs to be quantified to ensure that the Cl_2 will be available to react with the Hg.

Experimental Apparatus and Methods

All Cl_2 absorption experiments were performed at ambient temperature in the well-characterized stirred-cell contactor

with Teflon surfaces shown in Figure 1. Teflon tubing, fittings, and valves were used for all the connections. Mass flow controllers are labeled "FC."

Stirred-cell Reactor Apparatus

The stirred-cell contactor allowed gas/liquid contact, for which mass transfer properties were known or measured, at a known interfacial area (A) of $8.1 \times 10^{-3} \text{ m}^2$. The cylindrical reactor had a 0.01 m inner diameter and 0.016 m height. The reactor vessel consisted of a thick glass cylinder with Teflon-coated 316 stainless steel plates sealed to the top and bottom by thick gasket clamps. Four equally spaced, Teflon-coated, 316 stainless steel baffles were welded to the bottom plate. The baffles were long enough to extend to the main body of the gas phase. The bottom plate contained ports for liquid inlet and outlet. The top plate contained ports for the gas inlet and outlet, solution injection, and pH probe. The total volume of the reactor was $1.295 \times 10^{-3} \text{ m}^3$.

The stirred-cell contactor was equipped with independently controlled Teflon-coated agitators for gas- and liquid-phase mixing. The gas inlet was near the center of the top plate, directly above the gas agitator blade, to ensure that the inlet gas was properly mixed. Gas and liquid agitation speeds were measured using a tachometer. The mass transfer coefficients (k_g , k_L^o) were a function of the agitation rates.

Gas Source and Flow Path

Gas feed was prepared by quantitatively mixing 0.1% Cl_2 (1000 ppm in N_2) with N_2 . The Cl_2 cylinder was supplied by Air Products. The flow rates of all gas streams were controlled by Brooks mass flow controllers. The synthesized gas stream, typically at a flow rate of 1.2 L/min, was continuously fed to the reactor. After exiting the reactor, the gas stream was diluted with house air and continuously analyzed for Cl_2 . An empty 125-mL Erlenmeyer flask was connected after the reactor outlet to capture any water vapor or liquid. Since this flask stayed empty throughout an experiment, no liquid exited the reactor through the gas outlet. When the Cl_2 concentration to the reactor was less than 30 ppm, approximately 3 L/min of dilution air was used. When the Cl_2 concentration was greater, 36 L/min of dilution air was used. The Cl_2 analyzer output was connected to a strip chart recorder. The flux of Cl_2 was calculated from the gas-phase material balance. An analyzer with an electrochemical sensor (NOVA Model 540P) was initially used. Later experiments used ion mobility spectrometry (IMS) (Molecular Analytics AirSentry 10-Cl2).

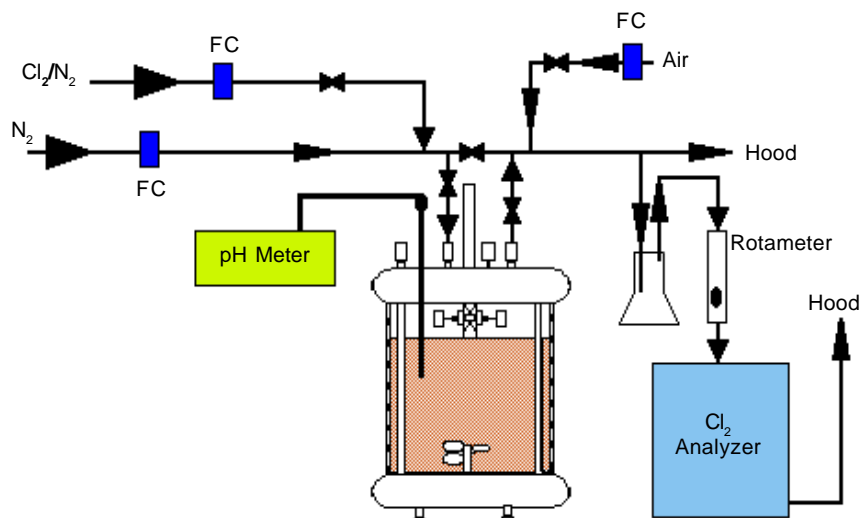


Figure 1. Stirred-cell Reactor Apparatus.

Analyzer Calibration

The Cl_2 analyzer was calibrated at the beginning and end of each experimental series to check for analyzer drift. There was essentially no drift for the IMS analyzer. During calibration, the gas flow rate was identical to that in an experiment. Other than bypassing the reactor, the gas flow path during calibration was the same as during an experimental run. To calibrate the analyzer zero, N_2 (without Cl_2) was supplied and diluted with house air. To calibrate the span, the gas flow rates were adjusted to give different Cl_2 concentrations spanning the range of interest.

Reactor Solution and Analysis

The reactor contained the aqueous S(IV) solution, ranging from 0 to 10 mM, used in absorbing Cl_2 . The reactor fluid volume in a typical experiment was $1.06 \times 10^{-3} \text{ m}^3$. Distilled water was first added to the reactor. For experiments at $\text{pH} \approx 4$, the reactor solution was buffered by injecting a stock solution of equimolar succinic acid/sodium succinate. The buffer concentration in the reactor ranged from 5 to 50 mM total succinate. The S(IV) solution was obtained by injecting a stock solution containing equimolar sodium sulfite and sodium bisulfite. For experiments at $\text{pH} > 7$, stock solutions of only sodium sulfite were used. Liquid samples were periodically taken from the bulk of the reactor and analyzed for S(IV) concentration by iodometric titration, and some

samples were analyzed for chloride using ion chromatography. The pH of the bulk reactor solution was continuously monitored and recorded using a strip chart recorder. In the buffered experiments, essentially all of the S(IV) was present as bisulfite since the pH was much lower than the pK_a of the sulfite/bisulfite reaction.

Iodometric Titration for S(IV)

After the S(IV) sample was withdrawn from the reactor, it was directly injected into excess iodine solution to avoid air oxidation to sulfate. The S(IV) reduced the iodine to iodide. The excess iodine was titrated with sodium thiosulfate. When the yellow color of the iodide started to fade (as the iodine was reduced to iodide by the thiosulfate), a couple drops of starch indicator were added to enhance the endpoint detection. The endpoint was reached when the blue solution turned clear.

The S(IV) concentration was determined from the difference between the amount of thiosulfate used to titrate the excess iodine and the amount needed if no S(IV) were added to the iodine. The difference indicates how much of the iodine reacted with S(IV).

Discussion of Results

The rate constant for the Cl_2 /S(IV) reaction was extracted from Cl_2 absorption data using the model for mass transfer with

fast irreversible reaction in the boundary layer. However, a precise value for the rate constant could not be determined due to the rapid reaction rate. The data were used to quantify an approximate value for the rate. The implications of the effect of this rate constant on Hg removal in a typical limestone slurry scrubber are examined.

Rate of Reaction for Cl_2 with S(IV)

Figure 2 depicts the chlorine flux as a function of the S(IV) concentration. The curves are calculated using the model for mass transfer with fast irreversible reaction in the boundary layer.

$$N_{Cl_2} = \frac{P_{Cl_2,i}}{H_{Cl_2}} \sqrt{D_{Cl_2} (k_{2,S(IV)} [S(IV)]_i + k_{2,buf} [buffer])} \quad (1)$$

The partial pressure of Cl_2 at the interface and the S(IV) concentration at the interface can be related to the bulk Cl_2 and S(IV), respectively.

$$F = D_{Cl_2} \left\{ k_{2,S(IV)} \left([S(IV)]_b - \frac{N_{Cl_2}}{\phi k_{L,S(IV)}} \right) + k_{2,buf} [buffer] \right\}$$

and

$$N_{Cl_2} = \frac{1}{H_{Cl_2}} \left(P_{Cl_2,b} - \frac{N_{Cl_2}}{k_g} \right) \sqrt{F} \quad (2)$$

The partial pressure of Cl_2 in the bulk (which is equivalent to the Cl_2 exiting the reactor) can be written in terms of the inlet Cl_2 concentration through a gas-phase material balance. Thus, Equation 3 displays the model used to calculate the curves, and Table 1 lists the parameters that were supplied to the model.

$$N_{Cl_2} = \frac{1}{H_{Cl_2}} \left(P_{Cl_2,in} - \frac{N_{Cl_2} A}{G} - \frac{N_{Cl_2}}{k_g} \right) \sqrt{F} \quad (3)$$

The rate constant of the Cl_2 /S(IV) reaction ($k_{2,S(IV)}$) was chosen to best fit the data. All the data plotted below were obtained through IMS analysis. The data at 0.01 mM S(IV) are actually in succinate buffer with no S(IV). The inverted triangles in Figure 2 represent points in which 15 to 20% oxygen was added. All the data are in 50 mM buffer except for the points represented by the squares with diagonal lines which are in 5 mM buffer.

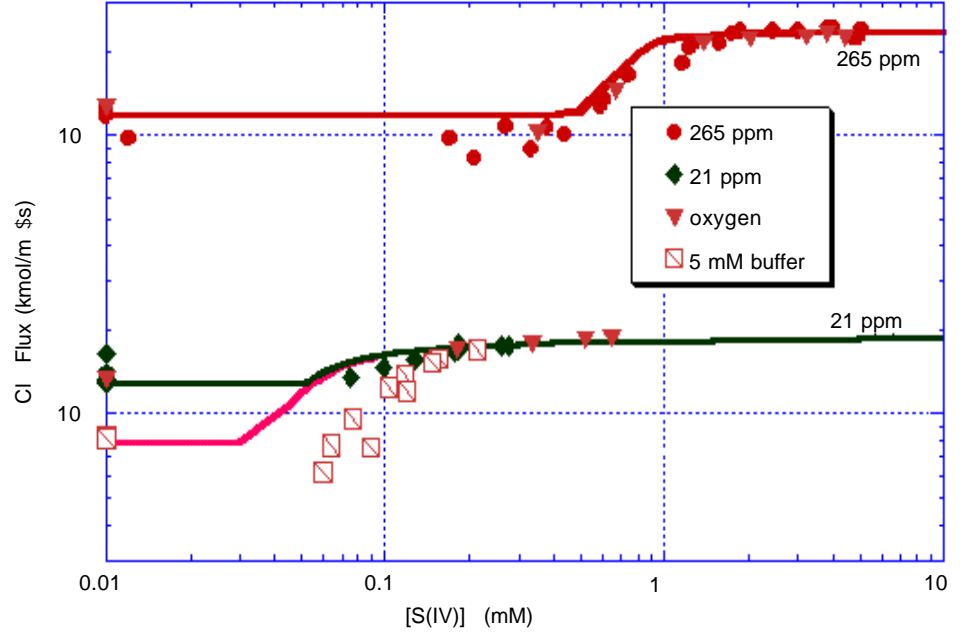


Figure 2. Chlorine Absorption in Buffered S(IV), $k_{2,S(IV)} = 2 \times 10^9$ L/mol \cdot s.

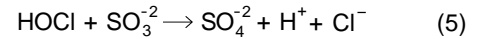
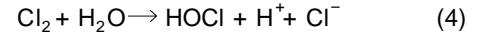
Table 1. Values of parameters in global model.

| Parameter | Units | Value |
|-----------------|------------------------------|-----------------------|
| D_{Cl_2} | m^2/s | 1.5×10^{-9} |
| G | m^3/s | 0.0708 ^a |
| ϕ | | 1 |
| H_{Cl_2} | $atm \cdot m^3/kmol$ | 16.7 |
| k_g | $kmol/s \cdot atm \cdot m^2$ | 0.00075 |
| $k_{L,S(IV)}^o$ | m/s | 2.45×10^{-5} |
| $k_{2,S(IV)}$ | $L/mol \cdot s$ | 2×10^9 |

^a 1.18 L/min

Figure 2 shows that, at high S(IV), the Cl_2 flux does not depend on the S(IV) concentration since the limit of gas film resistance is approached. At low S(IV), the flux is limited (in some cases inhibited) by the buffer-enhanced Cl_2 hydrolysis reaction. In this region, the flux depends only on the buffer reaction rate. However, the data show that, when very little S(IV) was injected, the Cl_2 flux was less than what it was initially in buffer alone. Thus, S(IV) inhibited Cl_2 absorption at very low S(IV) concentrations. As the S(IV) increased, the chlorine flux increased until the limit of gas film resistance was reached.

Since HOCl reacts with sulfite, one possible mechanism for Cl_2 reaction with S(IV) is that the Cl_2 first hydrolyzes in water to form HOCl, and then the HOCl (not Cl_2 directly) reacts with S(IV). These overall reactions are:



If this were the case, the rate of Cl_2 absorption in S(IV) would be equivalent to the rate of Cl_2 hydrolysis to form HOCl since Cl_2 hydrolysis is the rate-limiting step. Then, the HOCl would react with S(IV). However, since the addition of S(IV) results in a greater Cl_2 removal rate than the Cl_2 hydrolysis rate, it must not depend on HOCl formation. Thus, Cl_2 itself reacts with S(IV) directly, and it is not necessary for HOCl to form before Cl_2 reaction with S(IV) occurs.

In the intermediate region of Figure 2, the flux is limited by S(IV) diffusion to the interface [depicted by flux increasing linearly with S(IV)] and/or kinetics (depicted by curvature). Looking at the 265 ppm data, for S(IV) between 0.5 and 0.8 mM, the flux increases linearly with S(IV), which is consistent with the model of S(IV) depletion. At the lower inlet concentration of 21 ppm, the data do not fall on the model curve at S(IV) concentrations below 0.1 mM. These deviations result from

the experimental uncertainty in the S(IV) concentration measurements at low S(IV). For example, if the iodometric analysis yielded a S(IV) concentration of 0.07 mM, the actual value could be 0.03 mM due to the inaccuracies of analysis at low S(IV) concentration. Figure 2 shows that there is only a very small range (depicted by curvature) where the Cl₂ flux should be limited by the kinetics of the Cl₂/S(IV) reaction.

Even though it was difficult to obtain an exact value for the rate constant because of the mass transfer limitations of the reactor, an approximate value can easily be determined. Model curves were calculated for various rate constants to determine the value that best fitted the data. Instead of plotting flux as a function of bulk S(IV) as was done in Figure 2, plotting Cl₂ penetration ($Cl_{2,out}/Cl_{2,in}$) as a function of $[S(IV)]_b/P_{Cl_{2,in}}$ magnifies the errors in the data. This allows better observation of which value for $k_{2,S(IV)}$ best fits the data. Figure 3 plots the same data, without separately labeling the points with oxygen, and uses the same model as in Figure 2. The points on the y-axis do not contain any S(IV).

The model curves were calculated with rate constants ranging from 2.5×10^5 L/mol\$s to infinity. The rate constant used in Figure 3 fits the data better than the other rate constants used. Thus, the most probable value of the rate constant is 2×10^9 L/mol\$s, although it could be an order of magnitude smaller or larger. Many of the low S(IV) points, especially for the 21 ppm data, do not fall on the curve, but that could be due to the inability to accurately measure low S(IV) concentrations. In order to get a more precise rate constant, an apparatus with higher mass transfer coefficients is needed so that the absorption falls in a region controlled by reaction kinetics instead of mass transfer.

Hg Removal in a Typical Limestone Slurry Scrubber

The expected Hg removal in a limestone slurry scrubber can be predicted using the extracted rate constant for the Cl₂/S(IV) reaction, a preliminary rate constant for Hg/Cl₂, and typical mass transfer characteristics for a scrubber. Table 2 tabulates the parameters used in the model. The value for $k_{2,S(IV)}$ at 55° C was estimated from the value at 25° C. The model must be supplied with a given Cl₂ inlet and a constant S(IV) concentration. The model accounts for the two simultaneous reactions occurring at the gas/liquid interface: the depletion of Cl₂ through reaction with S(IV) ($k_{2,S(IV)}$) and the reaction of Hg with Cl₂ ($k_{2,Hg}$). Figure 4 shows

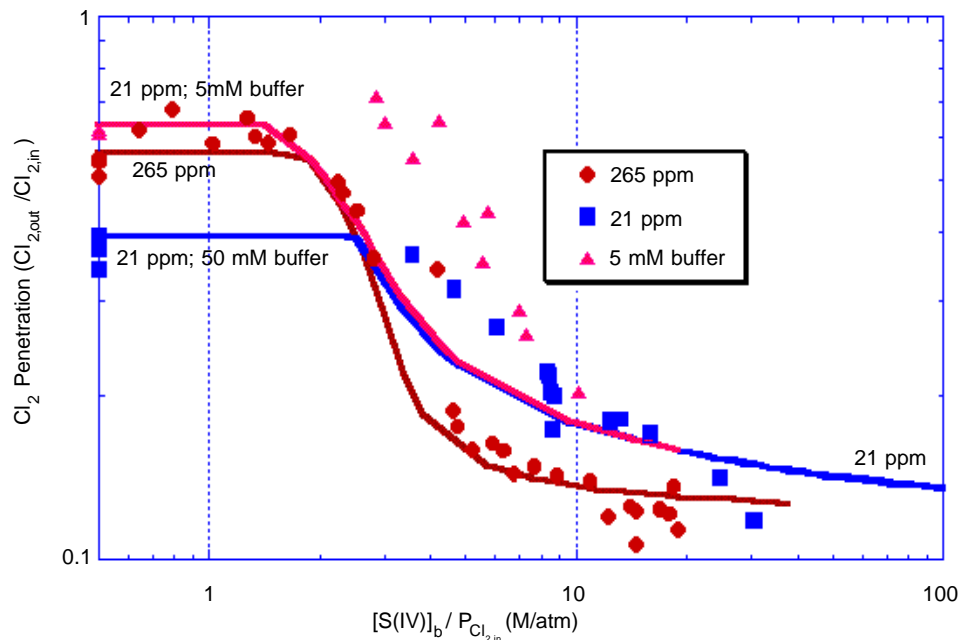


Figure 3. Chlorine Penetration in Buffered S(IV), $k_{2,S(IV)} = 2 \times 10^9$ L/mol\$\$.s.

Table 2. Parameters used to predict Hg removal.

| Parameter | Units | Value | |
|---------------|-----------------------------|-----------------------|-----------------------|
| | | 25° C | 55° C |
| $k_{2,S(IV)}$ | L/mol\$ | 2×10^9 | 2×10^{11} |
| $k_{2,Hg}$ | L/mol\$ | 1.7×10^{15} | 1.4×10^{17} |
| k_g | kmol/s\$atm\$m ² | 0.001 | 0.001 |
| D_{Cl_2} | m ² /s | 1.48×10^{-9} | 2.15×10^{-9} |
| D_{Hg} | m ² /s | 1.19×10^{-9} | 2.21×10^{-9} |
| H_{Hg} | atm\$m ³ /kmol | 8.91 | 35.64 |

the results of the model. The model curves were calculated at constant S(IV) of concentrations of 1 and 10 mM.

Mercury removal increases (penetration decreases) as the Cl₂ injected increases. Mercury removal decreases as S(IV) increases due to greater depletion of Cl₂ at the interface. At the higher temperature, there is less Cl₂ at the interface due to the higher reaction rate of Cl₂ with S(IV). However, since the reaction rate of Hg and Cl₂ also increases with temperature, significant Hg removal still occurs. Based on this model, only 1 ppm Cl₂ is needed to obtain 99% Hg removal. Since Cl₂ absorption is gas-film controlled,

99.9% chlorine removal will be achieved due to reaction with S(IV).

Conclusions

The rate constant for the Cl₂/S(IV) reaction was too rapid to be precisely measured using the stirred-cell reactor, due to mass transfer limitations. However, the most probable value for the rate constant was determined to be 2×10^9 L/mol\$\$. At low S(IV), the Cl₂ absorption was limited by the buffer-enhanced hydrolysis reaction. At moderate S(IV), it was limited by diffusion of S(IV) from the bulk solution to the interface. At high S(IV), the absorption was limited by diffusion of Cl₂ from the bulk gas to the interface.

Chlorine injection to enhance Hg removal may be feasible. In a typical limestone slurry scrubber, Cl₂ absorption will be gas-film controlled because of the rapid Cl₂/S(IV) reaction rate. Thus, 99 to 99.99% Cl₂ removal will be achieved in typical scrubbers. Also, there will be enough Cl₂ at the interface to react with Hg. The model shows that only 1 ppm Cl₂ is needed to get 99% Hg removal.

The succinate buffer enhances Cl₂ absorption. However, lowering the succinate buffer concentration did not aid in extracting kinetics because there is not much of a range between the Cl₂ flux due to absorption in water and the maximum flux resulting from complete gas-film control. Therefore, extracting kinetics for the S(IV)

reaction will always be difficult in the existing apparatus. On one end, absorption is limited by the Cl_2 hydrolysis reaction, and on the other end, it is limited by gas-film control in the stirred-cell contactor.

Chloride does not affect Cl_2 absorption in S(IV) since the $\text{Cl}_2/\text{S(IV)}$ reaction is irreversible. Oxygen does not affect Cl_2 absorption in S(IV) either, nor does it seem to catalyze S(IV) depletion at the ranges investigated.

Recommendations

In order to accurately predict Hg and Cl_2 removal in a scrubber, a better model with precise kinetics is needed. The $\text{Cl}_2/\text{S(IV)}$ reaction rate needs to be precisely measured in a gas/liquid contactor with higher mass transfer coefficients. Furthermore, this reaction rate should be measured at 55°C to simulate a typical limestone slurry scrubber.

Simultaneous absorption of Hg and Cl_2 must be measured and modeled to obtain a precise value for $k_{2,\text{Hg}}$. These experiments should also be done at 55°C . Simultaneous absorption of Hg, Cl_2 , and SO_2 should also be studied. Furthermore, in order to completely simulate flue gas, CO_2 , nitrogen oxides, and oxygen should be added to the inlet gas.

Results have shown that chloride does not affect Cl_2 absorption. However, experiments were not done in sodium chloride solutions higher than 0.02 M. Limestone slurry may have 1 M Cl^- . Thus, absorption into 1 M chloride must be quantified.

Nomenclature

A gas/liquid contact area (m^2)
 D_{Cl_2} diffusion coefficient for Cl_2 in water (m^2/s)
 D_{Hg} diffusion coefficient for Hg in water (m^2/s)

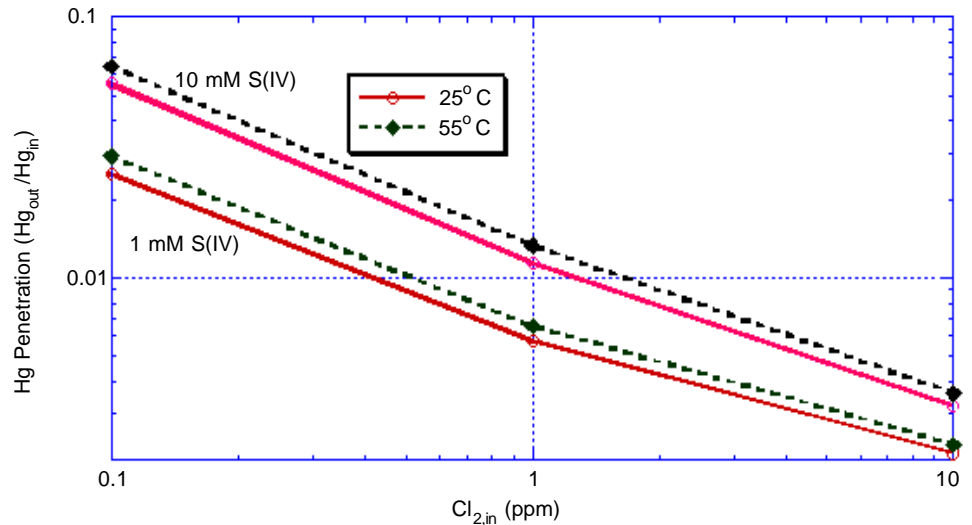


Figure 4. Predicted Hg Penetration.

| | | | |
|--------------------|--|----------------------|---|
| ϕ | reactant stoichiometric coefficient (dimensionless) | $k_{2,\text{Hg}}$ | second order rate constant for Hg/ Cl_2 reaction ($\text{L}/\text{mol}\cdot\text{s}$) |
| FC | Mass flow controller | $k_{2,\text{S(IV)}}$ | second order rate constant for $\text{Cl}_2/\text{S(IV)}$ reaction ($\text{L}/\text{mol}\cdot\text{s}$) |
| G | gas flow rate to reactor (m^3/s) | N_{Cl_2} | flux of Cl_2 ($\text{kmol}/\text{m}^2\cdot\text{s}$) |
| H_{Cl_2} | Henry's law constant for Cl_2 ($\text{atm}\cdot\text{m}^3/\text{kmol}$) | P_{Cl_2} | partial pressure of Cl_2 (atm) |
| H_{Hg} | Henry's law constant for Hg ($\text{atm}\cdot\text{m}^3/\text{kmol}$) | $\text{p}K_a$ | negative logarithm of acid dissociation constant |
| IMS | ion mobility spectrometry | [S(IV)] | concentration of S(IV) in liquid (M) |
| k_g | individual gas-film mass transfer coefficient ($\text{kmol}/\text{s}\cdot\text{atm}\cdot\text{m}^2$) | Subscripts | |
| k_L^o | individual physical liquid-film mass transfer coefficient (m/s) | b | in bulk |
| $k_{2,\text{buf}}$ | second order rate constant for Cl_2 /buffer reaction ($\text{L}/\text{mol}\cdot\text{s}$) | i | at gas/liquid interface |
| | | in | inlet |
| | | out | outlet |

S. Roy and G. Rochelle are with the Department of Chemical Engineering, The University of Texas at Austin, Austin, Tx 78712.

Theodore G. Brna is the EPA Project Officer (see below).

The complete report, entitled "Chlorine Absorption in S(IV) Solutions," (Order No. PB2001-107826; Cost: \$27.00, subject to change) will be available from:

National Technical Information Service

5285 Port Royal Road

Springfield, VA 22161-0001

Telephone: (703) 605-6000

(800) 553-6847 (U.S. only)

The EPA Project Officer can be contacted at:

Air Pollution Prevention and Control Division

National Risk Management Research Laboratory

U.S. Environmental Protection Agency

Research Triangle Park, NC 27711-0001

United States
Environmental Protection Agency
Center for Environmental Research Information
Cincinnati, OH 45268

Official Business
Penalty for Private Use
\$300

EPA/600/SR-01/054

PRESORTED STANDARD
POSTAGE & FEES PAID
EPA
PERMIT No. G-35